

Research Article

Role of fluorine doping on the electron transport layer of F-doped TiO₂ (Titanium dioxide) for photovoltaic systems and its environmental impact

Sweta

Department of Physics, Gurukula Kangri (Deemed to be University), Haridwar (Uttarakhand), India

Sagar Panwar

Department of Physics, Gurukula Kangri (Deemed to be University), Haridwar (Uttarakhand), India

Vinod Kumar

Department of Physics, The University of the West Indies - St. Augustine campus, Trinidad & Tobago

H. K. Malik

Department of Physics, Indian Institute of Technology, New Delhi, India

L. P. Purohit*

Department of Physics, Gurukula Kangri (Deemed to be University), Haridwar (Uttarakhand), India

*Corresponding author. E-mail: profppurohitphys@gmail.com; lppurohit@gkv.ac.in

Article Info

<https://doi.org/10.31018/jans.v16i3.5835>

Received: June 10, 2024

Revised: August 07, 2024

Accepted: August 13, 2024

How to Cite

Sweta, *et al.* (2024). Role of fluorine doping on the electron transport layer of F-doped TiO₂ (Titanium dioxide) for photovoltaic systems and its environmental impact. *Journal of Applied and Natural Science*, 16(3), 1189 - 1195. <https://doi.org/10.31018/jans.v16i3.5835>

Abstract

Photovoltaic (PV) systems are regarded as clean and sustainable energy sources and exhibit minimal pollution during their lifetime. The production of hazardous contaminants contaminating water resources, emissions of air pollutants during the manufacturing process, and the impact of PV installations on land use are important environmental factors to consider. The present study aimed to synthesise the F-doped Titanium dioxide (TiO₂) thin films on a glass substrate employing spin coating followed by the sol-gel process ETL application purpose. Fluorine-doped TiO₂ thin films were prepared using the sol-gel spin coating technique. The X-ray diffraction (XRD) results confirmed that the most intense peak was observed at 25.37° corresponding to the crystallographic plane (101) for anatase TiO₂. The average transparency of TiO₂ was increased by adding the doping level of fluorine and increment in the optical bandgap. The thickness of the thin film was kept at about 300 nm. The resistance of nanocrystalline thin films of different F doped TiO₂ was decreased from 1.322×10¹² Ω, 9.728×10¹¹ Ω, as the F doping concentration was increased from pristine to 7 at. %. Based on electrical measurements, it was observed that a suitable electron transport layer (ETL) of F-doped TiO₂ can be synthesized for photovoltaic applications. The present study offers a synthesis and analysis of F-doped TiO₂ that can be used to improve the sustainability of PV manufacturing processes, improve its economic value, and mitigate its negative impact on the environment.

Keywords: Electron transport layer, Environmental impact, F-doped TiO₂, Optical properties, Sol-gel preparation, Thin films

INTRODUCTION

The increase in the global population places heavy demands on the food, water, and energy sectors. Energy generation processes face major challenges such as sustainability, cost, security, and market price fluctuations. In addition, the increase in environmental awareness and the application of more stringent discharge regulations has directed the scientific community to work on developing alternative, sustainable, and renew-

able energy sources. With such implications, the transformation of energy systems has also received much attention, from focusing more on biofuels and solar cells. Hybrid and sustainable energy systems such as solar, wind, geothermal, and biomass are key technologies in the renewable revolution phase. Organic-inorganic hybrid perovskite solar cells (PSCs) based on halide perovskite material have proficient, unrivalled advancement in the last few years, showing appreciable potential for large-scale commercialization and ap-

plications (Xiang *et al.*, 2017). Titanium dioxide (TiO₂), as the most known electron transport layer (ETL) material, has been extensively adopted in PSCs due to its high transparency, carrier charge separation performance and environmental stability (Yang *et al.*, 2019). TiO₂ is an interesting material due to its different technological properties and ultimate applications involving energy-conversion applications such as photo-catalysis, fuel generation, CO₂ reduction, electrochromic devices and solar cells (Singh *et al.*, 2019). The non-toxicity, environmental compatibility and low price are other practical advantages of TiO₂ (Karthikeyan *et al.*, 2020). After so many applications, there is still a problem in commercial use, i.e., its wide band gap 3.2 eV; this large band gap makes it difficult to use in photocatalysis, solar cells, and other applications (Asemi *et al.*, 2017). There are a number of ways through which researchers have tried to reduce the band gap, such as doping, dye anchoring, heterogeneous composites (WO₃, SiO₂, Al₂O₃, etc.) and hybridization with nano-materials (Mathankumar *et al.*, 2020; Mishra *et al.*, 2020; Yahya *et al.*, 2018). Using non-metallic materials as dopants is a method to reduce band gaps with exceeding electrons coming from dopants. Nitrogen doping has always been the most attractive way to reduce the band gap (L. Tian *et al.*, 2013). Further, fluorine is another suitable candidate for doping in TiO₂ due to its effectiveness in generating more charge carriers, resulting in enhanced conductivity of the TiO₂ (Che *et al.*, 2017). In fact, phases such as anatase and rutile are present in TiO₂ nanocrystals, depending on preparation conditions. If the temperature is less than ~450°C, it may be an anatase phase; increasing temperature would lead to rutile phase (Upadhyay *et al.* 2021). Therefore, according application, researchers have been focused on optimum phase of TiO₂. The anatase phase is more stable as compared to rutile phase which is not good in different applications except photovoltaic application (Davis *et al.*, 2019).

Various deposition techniques are available to fabricate doped and undoped TiO₂ thin films like sol-gel spin coating technique, chemical vapour deposition, electrophoretic, screen printing, sputtering and electron beam deposition (Choudhary *et al.*, 2021). Among these, the sol-gel process is the most convenient as it is a low-cost, effective method for coating the films. The present study aimed to synthesize undoped and F-doped TiO₂ thin films by sol-gel spin coating technique for ETL application and to determine the effect of doping concentration on the structural, morphological, electrical, and optical properties of F-doped TiO₂ thin films.

MATERIALS AND METHODS

Thin films of undoped and F-doped TiO₂ were prepared on a glass substrate using the sol-gel spin coating technique

(Rajput *et al.*, 2018). The precursor solutions were prepared using titanium tetra isopropoxide (TTIP), and tri fluoroacetic acid as a source of Ti and F, respectively, while 2-methoxy ethanol was used as solvent. The TiO₂ solutions with F doping, such as 0, 1, 3, 5, and 7 at.%. were prepared separately and stirred 2 h at room temperature. After 24 h, the coating process on the glass substrate was started at the constant 2500 rate per minute for 30 s, dried at 200°C for 10 min with 10 layers, and annealed at 450°C for 60 min.

The crystalline properties of prepared thin films were analyzed by an X-ray diffractometer (Philips X'pert Pro-diffractometer) using CuK_α radiations (λ=0.15406 nm) (Upadhyay *et al.*, 2020). The optical property was analysed by UV-Vis-NIR spectrophotometer (Shimadzu, UV-3600) and electrical properties by two probe electrometers (Keithley-4200-SCS) at bias voltage in the range of -4 to +4 volt (Larumbe *et al.*, 2015).

RESULTS AND DISCUSSION

X-ray diffraction

The crystallinity of the F doped and undoped TiO₂ thin films using X-ray diffraction (XRD) pattern revealed the crystalline behavior of anatase TiO₂ as shown in Fig.1. The observed peaks exhibited the anatase TiO₂ phase (JCPDS No:-21-1272) and situated at 25.48°, 37.89°, 48.21°, 53.98°, and 55.23°, 62.98°, 69.05° correspond to the (101), (004), (200), (105), (211), (204) and (116) planes, respectively (Essalhi *et al.*, 2017). Fig.1 shows that the crystal structure of F doped TiO₂ thin films did not transform compared to undoped TiO₂ thin films (Sharma *et al.*, 2024). However, the intensities of the peaks along all (hkl) planes decreased as F doping content increased. Consequently, peaks were broadened also for higher doping content i.e. 7 at.%, which revealed that the crystallite size decreased with higher values of F. This might be due to the mismatch radius of F ion (0.136 nm) and Ti⁴⁺ (0.068 nm), and the crystallite size decreased due to the replacement of O₂ with F ions in the lattice site. Generally, X-rays reflect different angles from each plane and cause a broadening in the XRD peak (Kazeminezhad *et al.*, 2016). Although, there was no extra peak of any impurity in the form of Fluorine oxide, which revealed about successful doping in the TiO₂ lattice sites. The average crystallite size of thin films was calculated by using the well-known Debye-Scherrer's formula in equation (1) as follows (Panwar *et al.*, 2022):

$$D = \frac{0.9 \lambda}{\beta \cos \theta} \quad (1)$$

where, D refers average crystallite Size, β is full width at half maxima (FWHM) of the peak, λ is for X-ray wavelength (1.5406 Å) and q refers as diffraction an-

Table 1. Structural parameters of undoped and F-doped TiO₂ thin films

Sample (hkl):(101)	d-spacing (nm)	FWHM (degree)	Crystallite size (nm)	Strain $\epsilon \times 10^{-2}$
Pristine TiO ₂	0.3519	0.24512	33.2	6.03
F(1%)	0.3521	0.32764	24.8	8.05
F(3%)	0.3523	0.34753	23.4	8.54
F(5%)	0.3520	0.35323	23.0	8.68
F(7%)	0.3532	0.43856	18.6	10.78

gle. The average crystallite size of the pristine and F-doped TiO₂ thin films is mentioned in Table 1.

Surface morphology analysis

The surface morphology of the synthesized thin films of F-doped and undoped TiO₂ was examined via *Scanning Electron Microscope* (SEM) micrographs as shown in Fig. 2. SEM images (Fig. 2 a-c) showed that thin film formation was uniform or in-homogeneous by medium flaky nature morphology for undoped TiO₂ thin film and these flakes may be formed during the drying process in furnace due to surface tension between film and the air (Jeantelot *et al.*, 2018). However, the flaky nature

decreases in F(5%)-doped TiO₂ thin films and could exhibit better conductivity for this formation, as seen in Fig. 2 (d-f). Generally, capillary forces are generated during the drying process, which is responsible for the cracks in the film prepared by the spin coating technique.

Afterwards, the elemental composition of the prepared F-doped TiO₂ thin films determined using EDX is shown in Fig. 2 g and h. The EDX spectrum for pristine TiO₂ thin film is shown in Fig. 2 (g), while Fig. 2 (h) shows the elemental composition for F(5%)-doped TiO₂ thin film sample, which confirmed the presence of Ti, O and F owing to the successful doping during the

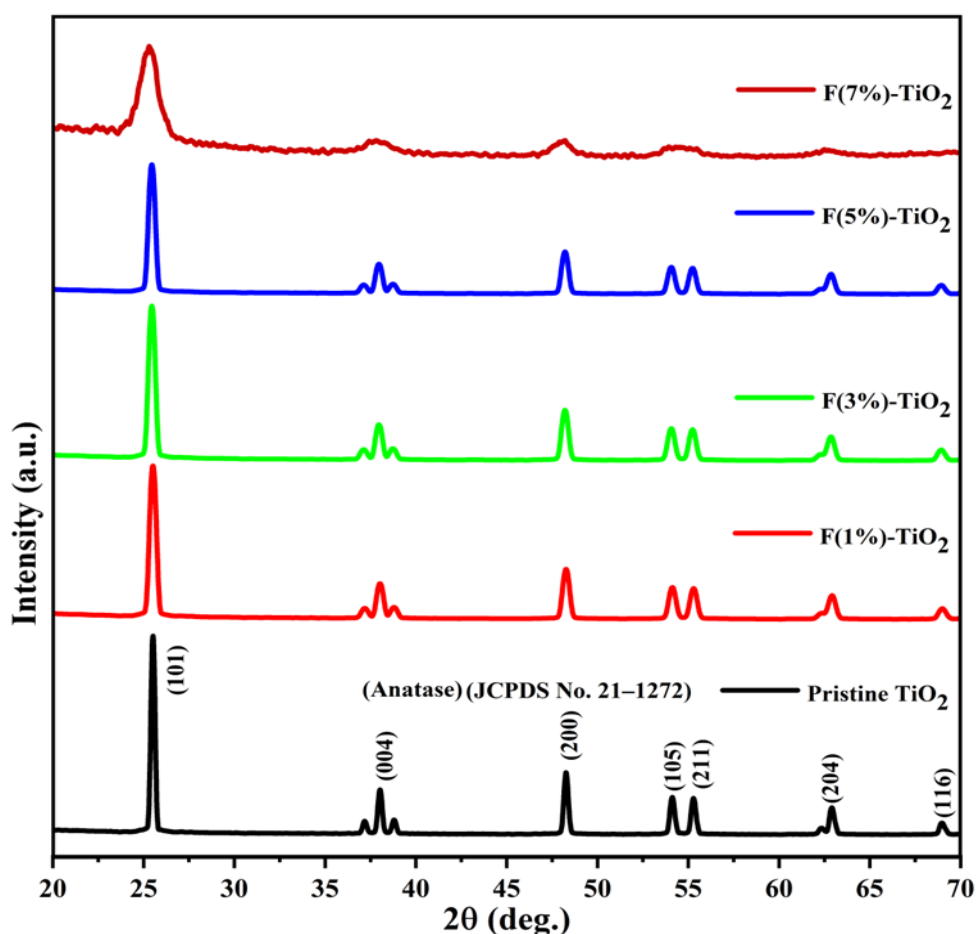


Fig.1. X-ray diffraction patterns shows the corresponding planes of undoped and F doped TiO₂ thin films matched with JCPDS card No. 21-1271

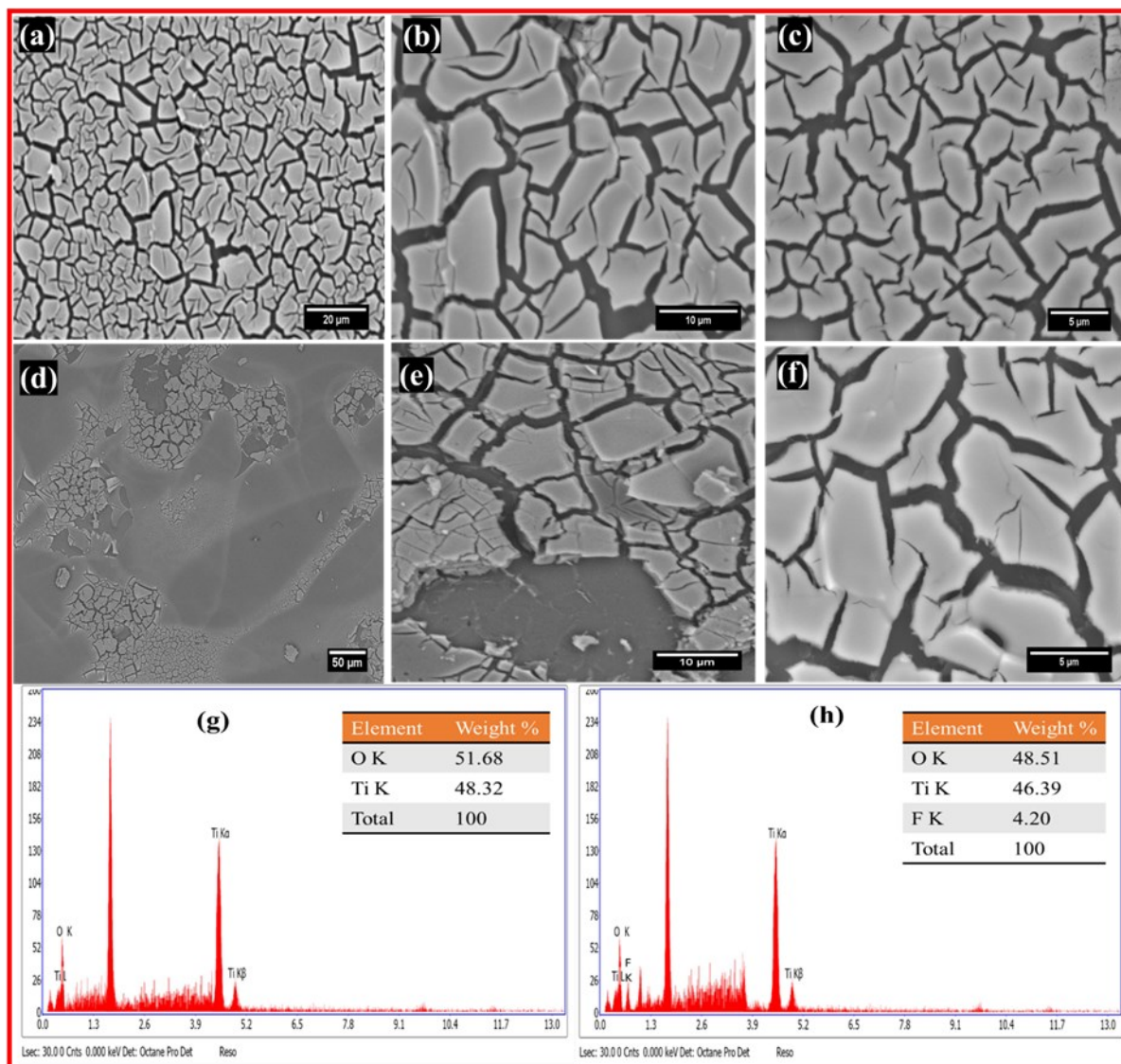


Fig.2. Scanning Electron Microscope (SEM) micrographs of undoped TiO₂ thin films at (a) 20 μm, (b) 10 μm, (c) 5 μm scale and F(5%)-doped TiO₂ at (d) 50 μm, (e) 10 μm, (f) 5 μm scales, (g) chemical elemental spectra for TiO₂ and (h) chemical elemental spectra for F(5%)-doped TiO₂ thin films

synthetization process. Therefore, doping TiO₂ with F can help reduce defects and recombination losses, improving solar cells' stability and longevity. Longer-lasting solar cells mean less frequent replacement and lower material waste and resource consumption.

Electrical measurements

The resistance of nanocrystalline thin films deposited on the glass substrate with various doping concentrations such as 0 at.%, 1 at.%, 3 at.%, 5 at.% and 7 at.% was found to be $1.322 \times 10^{12} \Omega$, $2.112 \times 10^{11} \Omega$, $5.807 \times 10^{10} \Omega$, $3.328 \times 10^9 \Omega$ and $9.728 \times 10^{11} \Omega$, respectively. As doping concentration was increased, an augmentation was observed in the resistance of F-doped TiO₂ thin films owing the lowest resistance with better conductivity as compared to pristine TiO₂ thin films (Wang *et al.*, 2021) as shown in Fig. 3(a).

Therefore, the minimum resistivity was observed for 5 at. % F doped TiO₂ thin films while maximum for pristine sample. This can be explained by SEM results because maximum oxygen vacancies formed by adding F in TiO₂ which were seen by white reflection in SEM as shown in Fig. 2 (f). Hence, the obtained minimum resistive thin films were further used to fabricate ETL for PV devices to provide maximum light-to-energy conversion. This could provide a sustainable and cheap PV device. F-doped TiO₂ ETLs can significantly enhance the efficiency of photovoltaic devices. Higher efficiency means more electricity is generated per unit area, potentially reducing the land and materials needed for solar power generation.

Ultraviolet-Vis study

The transmittance spectra were analyzed in the 300-

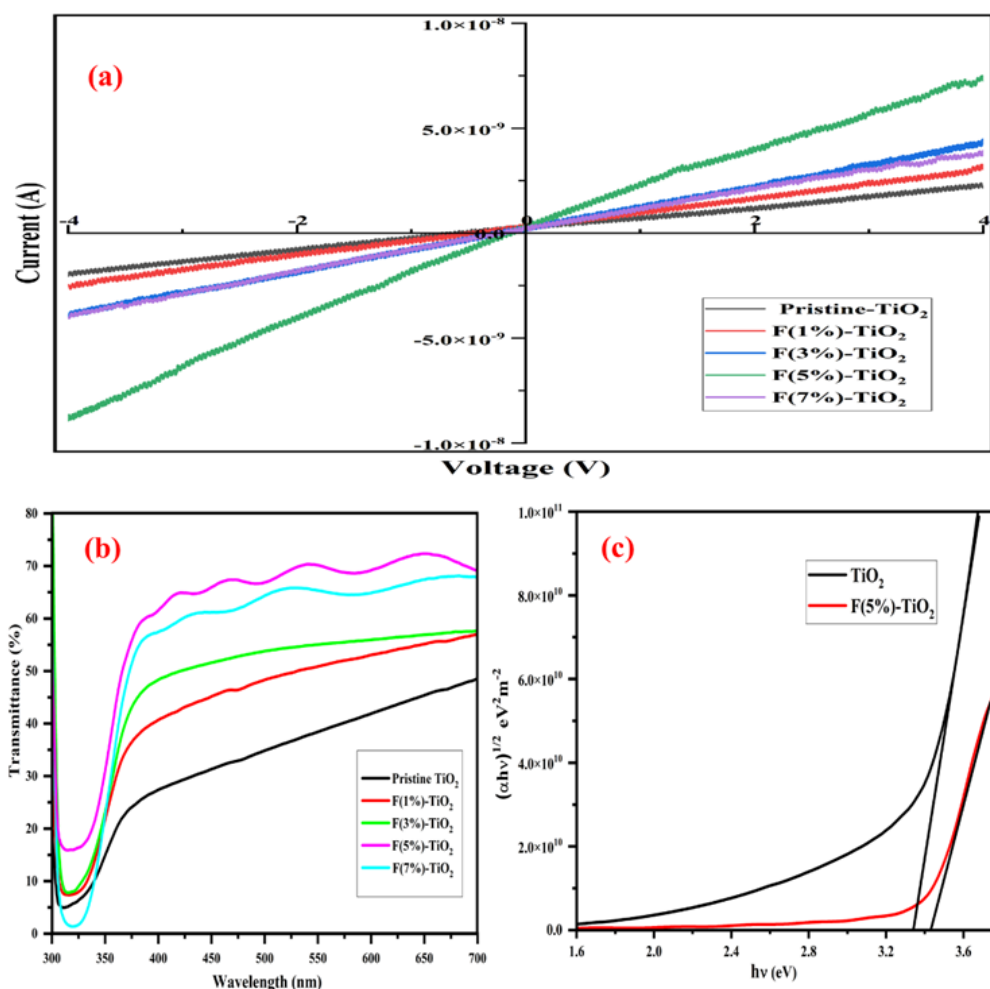


Fig.3. (a) I-V characteristics curve of F-doped TiO₂ thin films, (b) Transmittance of pristine and F-doped TiO₂ thin films within 300-700 nm and (c) Tauc's plot for pristine and F(5%)-doped TiO₂ thin films

700 nm wavelength range for all samples, as seen in Fig. 3(b). It is observed that the average transmittance was 35-70 % in the visible region for all samples. Moreover, the minimum transmittance value was found for TiO₂ films while the maximum for F-doped TiO₂ (5%). Thus 5% doping of fluorine in TiO₂ can be suitable for higher transmittance-based application (Al-Shomar, 2020). The absorption coefficient α is related to the direct band gap, which is function of frequency of light is indicated by the following formula (Tian *et al.*, 2013);

$$(\alpha h\nu) = A(h\nu - E_g)^{1/2} \quad (2)$$

where, E_g is the optical band gap, $h\nu$ is the photon energy, A is a constant independent of photon energy. Plotting the $(\alpha h\nu)^2$ versus $h\nu$, E_g was obtained by extrapolation method. The band gap of the fabricated thin films of pristine TiO₂ and F-doped TiO₂ is shown in Fig.3 (c). The band gap was increased with augmentation in F doping into TiO₂, which was calculated to be 3.32 eV and 3.56 eV, respectively which is suitable for ETL to manufacture PV devices. This blue shift was observed in the absorption edge with increasing the doping concentration of F into TiO₂. This may be relat-

ed to particle size, surface morphology, and variation with the increase in the doping concentration of F. This blue shift causes variation in the Fermi level of TiO₂ nanoparticles, leading to increased energy bandgap (Sharma *et al.*, 2021). Therefore, PV energy is a clean energy source, and its impact on air quality and climate change is significantly lower than that of any other traditional power generation system. Hence, it can assist in eliminating numerous environmental issues that result from utilizing fossil fuels. PV systems have zero emissions of carbon dioxide, methane, sulfur oxides, and nitrogen oxides during operation, which has negligible effects on air pollution and global warming.

Conclusion

TiO₂ thin films with different F-doping concentrations were prepared using the spin coating technique on glass substrates. It was observed that the crystallite size decreased as F doping content increased. Consequently, the flakiness of the films reduces and the film becomes more intact on the substrate surface. Through the optical analysis of the TiO₂ and F-doped TiO₂ thin

films, the transmittance increased as the F doping concentration increased. However, maximum transmittance was observed with 5 at.% doping of F and the band gap increased to 3.56 eV, making it appropriate to use F-doped TiO₂ as ETL in solar cells. The widespread solar energy facilities combined with efficient utilization promise to increase the energy supply and reduce the dependence on fossil fuels. However, the contribution of solar energy to the energy demand is still at the minimum level, and several economic and environmental challenges are faced.

Conflict of interest

The authors declare that they have no conflict of interest.

REFERENCES

- Al-Shomar, S. M. (2020). Investigation the effect of doping concentration in Ruthenium-doped TiO₂ thin films for solar cells and sensors applications. *Materials Research Express*, 7(3). <https://doi.org/10.1088/2053-1591/ab815b>
- Asemi, M., Maleki, S. & Ghanaatshoar, M. (2017). Cr-doped TiO₂-based dye-sensitized solar cells with Cr-doped TiO₂ blocking layer. *Journal of Sol-Gel Science and Technology*, 81(3), 645–651. <https://doi.org/10.1007/s10971-016-4257-z>
- Che, M., Fang, Y., Yuan, J., Zhu, Y., Liu, Q.m& Song, J. (2017). F-doped TiO₂ compact film for high-efficient perovskite solar cells. *International Journal of Electrochemical Science*, 12(2), 1064–1074. <https://doi.org/10.20964/2017.02.21>
- Choudhary, K., Saini, R., Upadhyay, G. K., Rana, V. S. & Purohit, L. P. (2021). Wrinkle type nanostructured Y-doped ZnO thin films for oxygen gas sensing at lower operating temperature. *Materials Research Bulletin*, 141 (March), 111342. <https://doi.org/10.1016/j.materresbull.2021.111342>
- Davis, K., Yarbrough, R., Froeschle, M., White, J. & Rathnayake, H. (2019). Band gap engineered zinc oxide nanostructures: Via a sol-gel synthesis of solvent driven shape-controlled crystal growth. *RSC Advances*, 9(26), 14638–14648. <https://doi.org/10.1039/c9ra02091h>
- Essalhi, Z., Hartiti, B., Lfakir, A., Mari, B., & Thevenin, P. (2017). Optoelectronics properties of TiO₂:Cu thin films obtained by sol gel method. *Optical and Quantum Electronics*, 49(9). <https://doi.org/10.1007/s11082-017-1142-0>
- Jeantelot, G., Ould-Chikh, S., Sofack-Kreutzer, J., Abou-Hamad, E., Anjum, D. H., Lopatin, S., Harb, M., Cavallo, L. & Basset, J. M. (2018). Morphology control of anatase TiO₂ for well-defined surface chemistry. *Physical Chemistry Chemical Physics*, 20(21), 14362–14373. <https://doi.org/10.1039/c8cp01983e>
- Karthikeyan, C., Arunachalam, P., Ramachandran, K., Al-Mayouf, A. M. & Karuppuchamy, S. (2020). Recent advances in semiconductor metal oxides with enhanced methods for solar photocatalytic applications. *Journal of Alloys and Compounds*, 828, 154281. <https://doi.org/10.1016/j.jallcom.2020.154281>
- Kazeminezhad, I., Saadatmand, S. & Yousefi, R. (2016). Effect of transition metal elements on the structural and optical properties of ZnO nanoparticles. *Bulletin of Materials Science*, 39(3), 719–724. <https://doi.org/10.1007/s12034-016-1206-y>
- Larumbe, S., Monge, M. & Gómez-Polo, C. (2015). Comparative study of (N, Fe) doped TiO₂ photocatalysts. *Applied Surface Science*, 327, 490–497. <https://doi.org/10.1016/j.apsusc.2014.11.137>
- Mathankumar, G., Bharathi, P., Mohan, M. K., Harish, S., Navaneethan, M., Archana, J., Suresh, P., Mani, G. K., Dhivya, P., Ponnusamy, S. & Muthamizhchelvan, C. (2020). Synthesis and functional properties of nanostructured Gd-doped WO₃/TiO₂ composites for sensing applications. *Materials Science in Semiconductor Processing*, 105(April 2019), 104732. <https://doi.org/10.1016/j.mssp.2019.104732>
- Mishra, A., Panigrahi, A., Mal, P., Penta, S., Padmaja, G., Bera, G., Das, P., Rambabu, P. & Turpu, G. R. (2020). Rapid photodegradation of methylene blue dye by rGO-V₂O₅ nano composite. *Journal of Alloys and Compounds*, 842, 155746. <https://doi.org/10.1016/j.jallcom.2020.155746>
- Panwar, S., Upadhyay, G. K., & Purohit, L. P. (2022). Gd-doped ZnO:TiO₂ heterogenous nanocomposites for advance oxidation process. *Materials Research Bulletin*, 145 (August 2021), 111534. <https://doi.org/10.1016/j.materresbull.2021.111534>
- Rajput, J. K., Pathak, T. K., Kumar, V., Swart, H. C., & Purohit, L. P. (2018). CdO:ZnO nanocomposite thin films for oxygen gas sensing at low temperature. *Materials Science and Engineering B: Solid-State Materials for Advanced Technology*, 228, 241–248. <https://doi.org/10.1016/j.mseb.2017.12.002>
- Sharma, H. K., Sharma, S. K., Vemula, K., Koirala, A. R., Yadav, H. M., & Singh, B. P. (2021). CNT facilitated interfacial charge transfer of TiO₂ nanocomposite for controlling the electron-hole recombination. *Solid State Sciences*, 112, 106492. <https://doi.org/10.1016/j.solidstatesciences.2020.106492>
- Sharma, H. K., Singh, B. P., & Sharma, S. K. (2024). CNT -TiO₂ nanocomposite thin films enhanced photocatalytic degradation of methylene blue. *Hybrid Advances*, 5, 100152. <https://doi.org/10.1016/j.hybadv.2024.100152>
- Singh, K., Harish, S., Archana, J., Navaneethan, M., Shimomura, M., & Hayakawa, Y. (2019). Investigation of Gd-doped mesoporous TiO₂ spheres for environmental remediation and energy applications. *Applied Surface Science*, 489, 883–892. <https://doi.org/10.1016/j.apsusc.2019.05.253>
- Tian, J., Gao, H., Deng, H., Sun, L., Kong, H., Yang, P., & Chu, J. (2013). Structural, magnetic and optical properties of Ni-doped TiO₂ thin films deposited on silicon(100) substrates by sol-gel process. *Journal of Alloys and Compounds*, 581, 318–323. <https://doi.org/10.1016/j.jallcom.2013.07.105>
- Tian, L., Giusti, G., Dan, C. Y., Cagnon, L., Volpi, F., Mantoux, A., & Daniele, S. (2013). *Characterization of Nitrogen-Doped TiO₂ Thin Films for Photovoltaic Applications*. 2479–2482.
- Upadhyay, G. K., Kumar, V., & Purohit, L. P. (2021). Optimized CdO:TiO₂ nanocomposites for heterojunction solar

- cell applications. *Journal of Alloys and Compounds*, 856, 157453. <https://doi.org/10.1016/j.jallcom.2020.157453>
21. Upadhyay, G. K., Rajput, J. K., Pathak, T. K., Swart, H. C., & Purohit, L. P. (2020). Photoactive CdO:TiO₂ nanocomposites for dyes degradation under visible light. *Materials Chemistry and Physics*, 253, 123191. <https://doi.org/10.1016/j.matchemphys.2020.123191>
22. Wang, H., Zhao, C., Yin, L., Li, X., Tu, X., Lim, E. G., Liu, Y., & Zhao, C. Z. (2021). W-doped TiO₂ as electron transport layer for high performance solution-processed perovskite solar cells. *Applied Surface Science*, 563(May), 150298. <https://doi.org/10.1016/j.apsusc.2021.150298>
23. Xiang, Y., Ma, Z., Zhuang, J., Lu, H., Jia, C., Luo, J., Li, H. & Cheng, X. (2017). Enhanced Performance for Planar Perovskite Solar Cells with Samarium-Doped TiO₂ Compact Electron Transport Layers. *Journal of Physical Chemistry C*, 121(37), 20150–20157. <https://doi.org/10.1021/acs.jpcc.7b05880>
24. Yahya, N., Aziz, F., Jamaludin, N. A., Mutalib, M. A., Ismail, A. F., Salleh, W. N., Jaafar, J., Yusof, N. & Ludin, N. A. (2018). A review of integrated photocatalyst adsorbents for wastewater treatment. *Journal of Environmental Chemical Engineering*, 6(6), 7411–7425. <https://doi.org/10.1016/j.jece.2018.06.051>
25. Yang, W., Wang, X., Li, H., Wu, J., Hu, Y., Li, Z. & Liu, H. (2019). Fundamental research on the effective contact area of micro-/nano-textured surface in triboelectric nanogenerator. *Nano Energy*, 57(December 2018), 41–47. <https://doi.org/10.1016/j.nanoen.2018.12.029>